Journal of Alloys and Compounds 889 (2021) 161623

Contents lists available at ScienceDirect

Journal of Alloys and Compounds

journal homepage: www.elsevier.com/locate/jalcom

Interparticle magnetic interactions in synthetic ferrihydrite: Mössbauer spectroscopy and magnetometry study of the dynamic and static manifestations

Yu.V. Knyazev[a,*], D.A. Balaev[a,b], S.V. Stolyar[a,b,c], A.A. Krasikov[a], O.A. Bayukov[a], M.N. Volochaev[a], R.N. Yaroslavtsev[a,c], V.P. Ladygina[c], D.A. Velikanov[a], R.S. Iskhakov[a]

[a] Kirensky Institute of Physics, Federal Research Center KSC SB RAS, Akademgorodok 50, bld. 38, Krasnoyarsk 660036, Russia
[b] Siberian Federal University, Svobodniy 79, Krasnoyarsk 660041, Russia
[c] Krasnoyarsk Scientific Center, Federal Research Center KSC SB RAS, Akademgorodok 50, Krasnoyarsk 660036, Russia

ARTICLE INFO

Article history:
Received 8 April 2021
Received in revised form 6 August 2021
Accepted 15 August 2021
Available online 16 August 2021

Keywords:
Ferrihydrite nanoparticles
Superparamagnetism
Interparticle magnetic interactions

ABSTRACT

Samples of synthetic ferrihydrite with an average nanoparticle size of 2.7 nm have been examined by magnetometry and Mössbauer spectroscopy. Ferrihydrite is characterized by the antiferromagnetic interactions between the magnetic moments of iron atoms. In ferrihydrite nanoparticles, as in any other antiferromagnetic ones, structural defects induce the formation of an uncompensated magnetic moment, which determines the magnetic properties typical of single-domain ferro- and ferrimagnetic particles. The manifestation of the magnetic interactions between ferrihydrite nanoparticles in the magnetic properties of the material and in the temperature evolution of Mössbauer spectra has been in focus. The results obtained on synthetic ferrihydrite have been compared with the data for the biogenic ferrihydrite sample with a similar average size of particles surrounded by a polysaccharide shell, which weakens and screens the interparticle magnetic interactions. A clear manifestation of the effect of the interparticle magnetic interactions on the transition to the blocked state is the presence of a significant contribution of the relaxation component in the Mössbauer spectra at temperatures of the transition from the superparamagnetic to blocked state. The temperature dependence of the particle relaxation time obtained from the Mössbauer spectra points out the collective effect of freezing of the magnetic moments of particles due to the magnetic interactions between them.

1. Introduction

Ferrihydrite is a hydrated ferric oxide with the nominal formula $Fe_2O_3{\cdot}nH_2O$, where the water content can be different [1,2]. This mineral exists only on the nanoscale and is widespread in water systems on the Earth's surface. It plays an important role in the vital activity of microorganisms and higher animals, which can be seen on the example is ferritin. Ferritin is a ferrihydrite nanocrystal encapsulated in a protein shell. It is responsible for storing iron in the living organism. Ferrihydrite is nontoxic to humans and animals [3,4] and currently used in anemia medicine. Due to the large fraction of the surface, which is characteristic of all nanoparticles, ferrihydrite is a good sorbent [5]. It can be obtained by chemical methods (synthetic (chemical) ferrihydrite) [6] or produced by microorganisms during the vital activity (bacterial (biogenic) ferrihydrite [7,8]).

The magnetic moments of iron atoms in ferrihydrite are ordered antiferromagnetically [9]. Seemingly, this type of ordering should classify ferrihydrite as a weak magnetic substance. Meanwhile, due to structural defects, fine antiferromagnetic (AFM) particles can acquire a fundamentally new property: uncompensated magnetic moment μ_{un} [10,11]. Obviously, this moment depends on a relative number of defects, or, to be exact, on their type. As was shown by Néel [12] using the statistical considerations, different μ_{un} values can be expected for three different types of defects: (i) $\mu_{un} \sim \mu_{at}{\cdot}N^{1/3}$ (μ_{at} is the magnetic moment of an atom and N is the number of magnetically active atoms in a particle) when defects only exist on the particle surface; (ii) $\mu_{un} \sim \mu_{at}{\cdot}N^{1/2}$ when there are defects distributed fairly uniformly both on the surface and in the bulk of a particle; and (iii) $\mu_{un} \sim \mu_{at}{\cdot}N^{2/3}$ for a prefect (defect-free) AFM particle with an odd

* Corresponding author.
E-mail addresses: yuk@iph.krasn.ru (Y.V. Knyazev), dabalaev@iph.krasn.ru (D.A. Balaev).

https://doi.org/10.1016/j.jallcom.2021.161623
0925-8388/

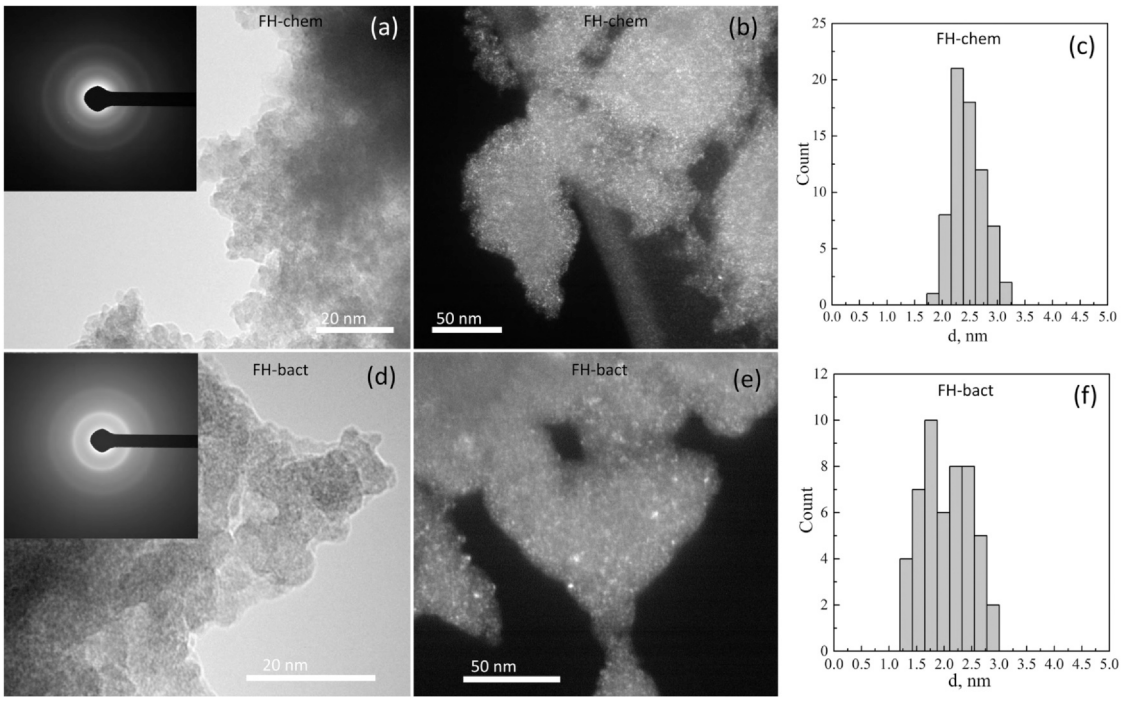

Fig. 1. (a, d) TEM images of chemical and biogenic ferrihydrite nanoparticles. Inset in (a, d): microdiffraction patterns. (b, e) Dark-field images of chemical and biogenic ferrihydrite nanoparticles. (c, f) Particle size distributions for the chemical and biogenic samples.

number of ferromagnetically ordered planes [12]. A simple estimation, even in intermediate case (ii) with $\mu_{un} \sim \mu_{at} \cdot N^{1/2}$, yields fairly large (hundreds of Bohr magnetons μ_B) μ_{un} values at $N \sim 10^3$ and $\mu_{at} \approx 5\ \mu_B$. Such values were determined when studying the magnetic properties of ferrihydrite and ferritin in [13–21]; in most cases, the ratio $\mu_{un} \sim \mu_{at} \cdot N^{1/2}$ was valid [13–19].

The above-mentioned values of the uncompensated magnetic moment of ferrihydrite nanoparticles already allow us to assign ferrihydrite to a class of magnetic nanoparticles, which makes it promising for application in various fields. The nontoxicity of ferrihydrite and its antibacterial properties [3] provide great opportunities for use of the magnetic properties of ferrihydrite nanoparticles in biomedicine; the first successful results have already been reported [22,23].

By now, there have been certain unsolved problems, both practical and fundamental, concerning the use of AFM nanoparticles, including ferrihydrite ones. Among these problems is the effect of the interparticle magnetic interactions on the behavior of a system of particles. In some fields of applications, when particles, for example, are immersed in a liquid in an external field, such interactions will inevitably lead to the undesirable coalescence of particles. For ferromagnetic (FM) and ferrimagnetic nanoparticles, the manifestation of interparticle interactions in different characteristics of a material were thoroughly investigated [24–40]. Although the magnetic moment of AFM nanoparticles is smaller ($\mu_{un} \sim 10^2\ \mu_B$) than that of single-domain FM particles ($\sim 10^3\ \mu_B$), some studies showed the effect of interparticle interactions on the magnetic properties of AFM nanoparticle systems [10,41–48].

The aim of this study was to examine synthetic ferrihydrite nanoparticles by magnetometry (the quasi-static magnetic properties) and Mössbauer spectroscopy (MS) in other to elucidate the impact of the interparticle magnetic interactions on the transition to the superparamagnetic (SPM), or unblocked, state of such systems. The focus of this work is on a chemical ferrihydrite sample. For comparison, the data on a reference sample of biogenic ferrihydrite produced by the vital activity of bacteria [7,8,18,49] are reported. The conditions for the cultivation of bacteria determine the presence of a polysaccharide shell on the ferrihydrite particle surface [50]. This ensures the spatial separation of particles and screening of their magnetic interactions.

2. Experimental

Chemical ferrihydrite (hereinafter, FH-chem) was synthesized at room temperature by slowly adding a sodium hydroxide (NaOH) solution (1 M) to a ferric chloride ($FeCl_3$) solution (0.02 M) until the neutral pH value under constant stirring. The alkali addition rate varied from 0.01 to 0.001 mol/min. The forming precipitate was collected on a filter, washed, and dried at room temperature.

A ferrihydrite biogenic sample was isolated from bacterial sediments after cultivation of *Klebsiella oxytoca* bacteria under anaerobic conditions [7,8,18]. The obtained dried sol is an aggregated system of ferrihydrite nanoparticles coated with an organic shell [50] with an average size of 2–3 nm. The samples from different series obtained by this technique have the identical particle sizes and, according to the static magnetic measurements, their characteristic SPM blocking temperatures are 15–25 K. The investigated biogenic ferrihydrite sample are hereinafter referred to as FH-bact.

The electron microscopy and microdiffraction investigations were carried out on a Hitachi HT7700 transmission electron microscope at an accelerating voltage of 100 kV. Specimens were prepared by shaking the nanoparticle powder in alcohol in an ultrasonic bath and depositing the obtained suspension onto support meshes with a perforated carbon coating.

The temperature dependences of the magnetization M(T) were measured on a SQUID magnetometer in external fields of 1–100 Oe [51] and a vibrating sample magnetometer [52] in fields of 1−50 kOe in the zero-field cooling (ZFC) and field cooling (FC) modes. The field dependences of magnetization M(H) were measured up to maximal magnetic field of 60 kOe.

The Mössbauer spectra of the sample were obtained on an MS-1104Em spectrometer (Research Institute of Physics, Southern Federal University) in the transmission geometry with a Co^{57}(Rh) radioactive source in the temperature range of 4–300 K using a

CFSG-311-MESS cryostat with a sample in the exchange gas based on a closed-cycle Gifford–McMahon cryocooler (Cryotrade Engineering). The spectra were processed by varying the entire set of hyperfine parameters using the least squares method in the linear approximation. The Mössbauer relaxation spectra were fitted using a two-stage relaxation model [53,54].

3. Results

3.1. Microstructural and Magnetic Characterization

Fig. 1 presents the results of the microstructural study of the ferrihydrite samples, including typical micrographs, microdiffraction patterns, and size distributions of particles. The microdiffraction patterns contain two diffusion reflections corresponding to interplanar spacings of 1.5 and 2.6 Å. We used the Scherrer's formula to determine the average particle size in the two samples. This method takes into account the broadening of diffraction reflections due to the size effects. To obtain the average particle size, a half-width of the first brightest diffraction ring was examined. Our estimation yielded < d > values of 2.8 and 2.4 nm for samples FH-chem and FH-bact, respectively. Then, a set of particles was treated to obtain the particle size histograms. We evaluated the particle size distributions by the micrographs using conventional computer tools. The histograms shown in Fig. 1c,f for the two samples are similar. The measured average particle sizes < d > were 2.7 and 2.2 nm for samples FH-chem and FH-bact, respectively, which is consistent with the Scherrer's formula estimation.

Fig. 2 shows temperature dependences of the magnetization for the samples measured in an external field of H = 100 Oe in the ZFC and FC modes. These dependences can be considered, in the first approximation, typical of systems of magnetic nanoparticles: at high temperatures, particles are in the SPM state (the thermomagnetic prehistory does not affect the magnetization) and, at low temperatures, the magnetic moments of particles are blocked, which is accompanied by the effect of the magnetic prehistory. The investigated samples exhibit a difference between the temperatures of the $M(T)_{ZFC}$ maxima and between the behaviors of the $M(T)_{FC}$ dependences. This will be is discussed in detail in Section 3.2.

At low temperatures, the M(H) curves exhibit a hysteresis, which can be seen in Fig. 3a for sample FH-chem. The M(H) isotherms in the region of the SPM state are also shown. As is known, the M(H) dependence for AFM nanoparticles can be described, in the first approximation, by the equation [10,13,16–21,55–67].

$$M(H) = M_{FM}(H) + \chi \cdot H \cdot \quad (1)$$

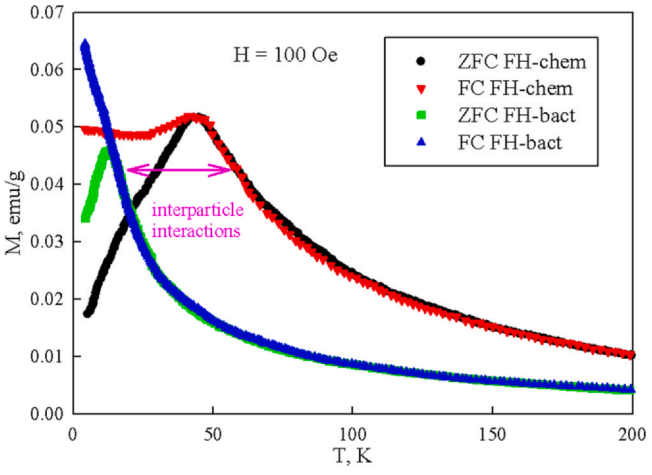

Fig. 2. FC and ZFC temperature dependences of the magnetization obtained in a field of H = 100 Oe for the biogenic (FH-bact) and chemical (FH-chem) ferrihydrite samples.

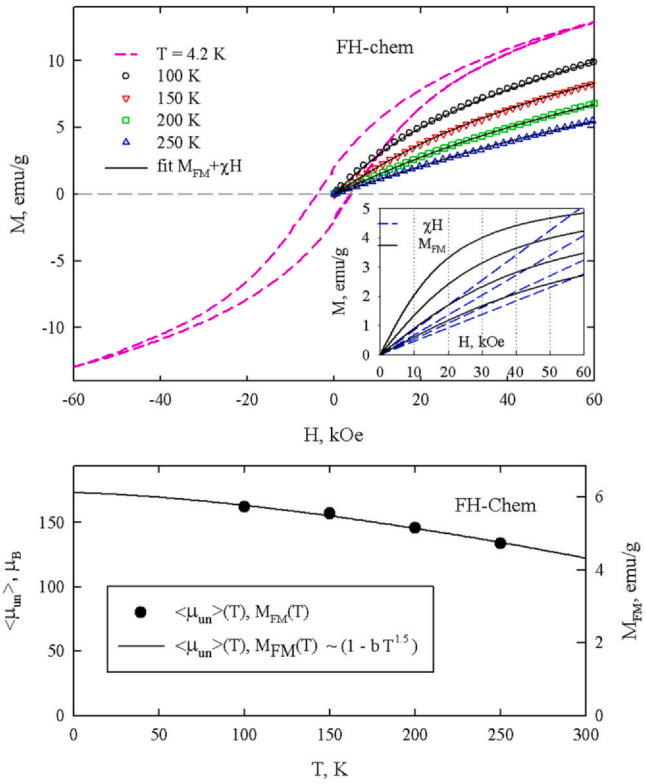

Fig. 3. (a) M(H) dependences for sample FH-chem at different temperatures. For the data obtained at T = 100 K and higher, symbols correspond to the experiment and solid lines are the results of the best fitting by Eq. (2). Inset in (a): partial components of the fitting curves. (b) Temperature dependence of the average magnetic moment of particles according to the fitting results (symbols).

Here, $M_{FM}(H)$ is the contribution of uncompensated magnetic moments μ_{un} of particles and χ is the AFM susceptibility of a material and other contributions [10,15–17,55–62]. In the SPM state, the first term in Eq. (1) is conventionally simulated by the Langevin function $L(\mu_{un}, H) = \coth(\mu_{un} \times H / kT) - 1/(\mu_{un} \times H/kT)$ (k is the Boltzmann constant); in addition, it is necessary to take into account the distribution of the μ_{un} values (the $f(\mu_{un})$ function) [14,17,19,21,63–66]. Therefore, Eq. (1) is rewritten in the following form

$$M(H) = N_P \int_0^\infty L(\mu_{un}, H) f(\mu_{un}) \mu_{un} \, d\mu_{un} + \chi H \quad (2)$$

In processing the M(H) dependences, $f(\mu_{un})$ is conventionally the lognormal distribution $f(\mu_{un}) = (\mu_{un} \cdot s \cdot (2\pi)^{1/2})^{-1} \exp\{-[\ln(\mu_{un}/n)]^2 / 2s^2\}$ with the average particle magnetic moment $< \mu_{un} > = n \cdot \exp(s^2)$, where s^2 is the $\ln(\mu_{un})$ dispersion. Assuming that the parameters N_P (the number of particles per unit sample mass) and s (the best agreement was obtained at $s^2 = 0.1$) do not change with temperature [17–19,66] and the fitting parameters are only the n values (the n value determines $< \mu_{un} >$) and χ, we fitted the experimental M(H) dependences in Fig. 3a by Eq. (2). The partial components $M_{FM}(H)$ and $\chi \cdot H$ of this fitting are shown in the inset in Fig. 3a.

Fig. 3b presents the temperature evolution of the uncompensated magnetic moment $< \mu_{un} > (T)$. It satisfactorily obeys the law $< \mu_{un} > (T) = < \mu_{un} > (T = 0) \cdot (1 - b \cdot T^{1.5})$, which allows us to obtain, with good accuracy, the value $< \mu_{un} > (T = 0) \approx 174 \ \mu_B$. The observed $< \mu_{un} > (T)$ dependence and the obtained $< \mu_{un} > (T = 0)$ value are characteristic of ferrihydrite [16–19,37,66]. Therefore, the investigated chemical ferrihydrite sample has the magnetic characteristics typical of such systems and the results obtained below can be confidently considered inherent in these materials. The quantity $< \mu_{un} > (T = 0) \approx 174 \ \mu_B$ corresponds to ~35 uncompensated moments of Fe^{3+} atoms (at $\mu_{at} = \mu_{Fe} = 5 \ \mu_B$) in a particle, which is consistent with

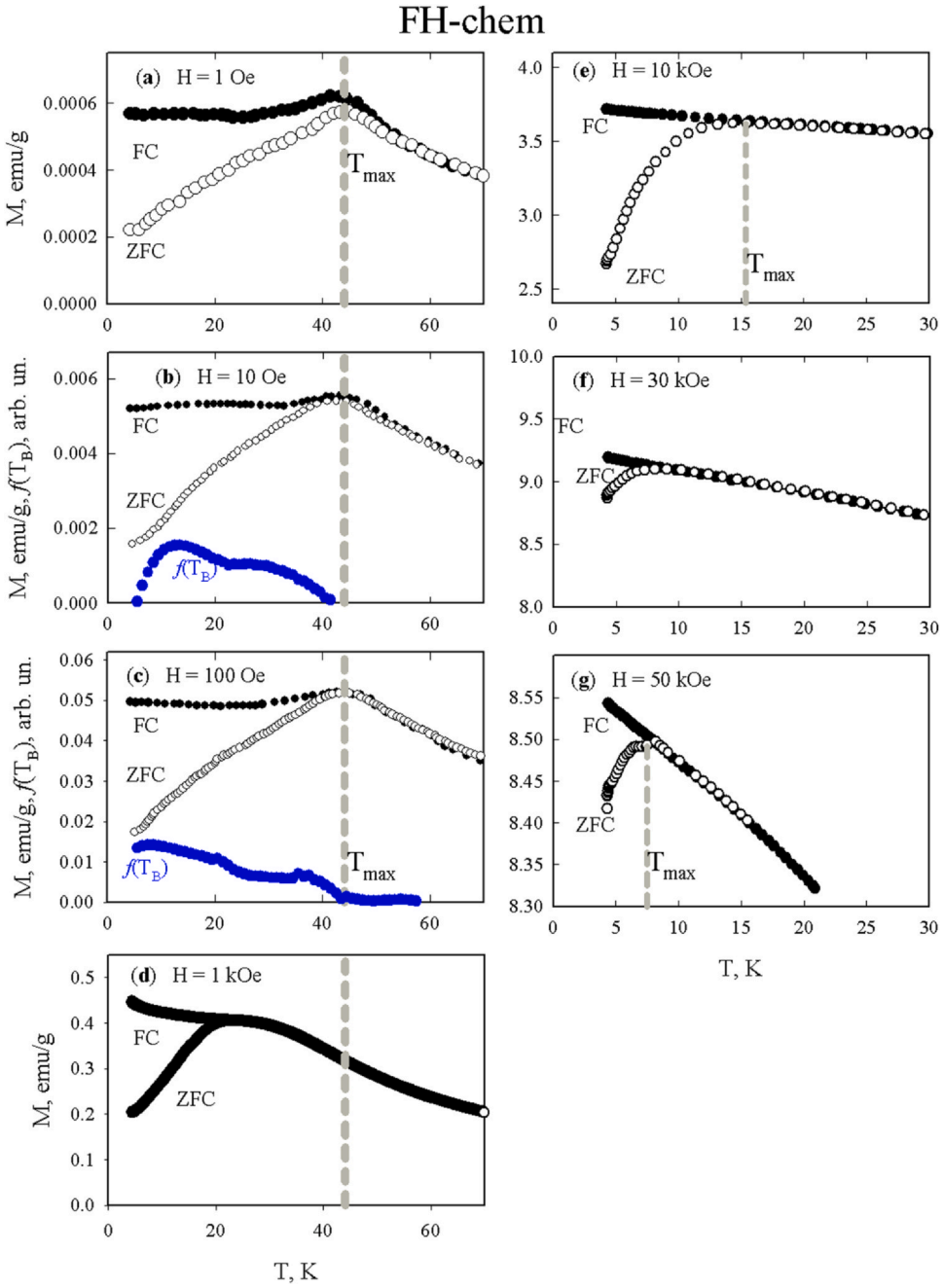

Fig. 4. FC and ZFC M(T) dependences for sample FH-chem in different fields H. Vertical dashed lines correspond to temperatures T_{max} in the $M(T)_{ZFC}$ dependences. (b, c) Dependences $f(T_B) \sim d(M(T)_{ZFC} - M(T)_{FC}/dT)$ (arbitrary units).

the Néel hypothesis for case (ii), i.e., at $\mu_{un} \sim \mu_{at} \cdot N^{1/2}$ (there are defects on the surface and in the bulk of a particle); at $< d > \approx 2.7$ nm, we obtain $N \approx 10^3$ and $N^{1/2} \approx 30$.

A similar analysis of the magnetization curves in the SPM state for the biogenic ferrihydrite samples was performed in [18,19,66]. The $< \mu_{un} > (T = 0)$ values for the samples from different series lied in the range of $(160–200)\mu_B$ with an average particle size of 2–3 nm, which, taking into account the polysaccharide shell on the particle surface [50], allows us to compare the data on biogenic ferrihydrite with the results obtained for the synthetic ferrihydrite sample, considering sample FH-bact to be reference, with the very weak effect of the interparticle magnetic interactions.

3.2. Evolution of the M(T) dependences in different external fields

Figs. 4 and 5 show the M(T) dependences obtained in different fields under the FC and ZFC conditions for samples FH-chem and FH-bact. Comparing the data in Figs. 4 and 5, we can distinguish two features indicative of a difference between the chemical and biogenic ferrihydrite samples.

The first feature is related to the effect of an external field on temperature T_{max} corresponding to the $M(T)_{ZFC}$ maximum. In sample FH-chem, the temperature T_{max} does not change with an increase in the magnetic field from 1 Oe to 1 kOe ($T_{max} \approx 44$ K). Only in external fields of H = 10, 30, and 50 kOe, the characteristic temperature T_{max} shifts toward lower temperatures. In sample FH-bact (Fig. 5), the T_{max} value monotonically decreases from 13.7 to 9.5 K with an

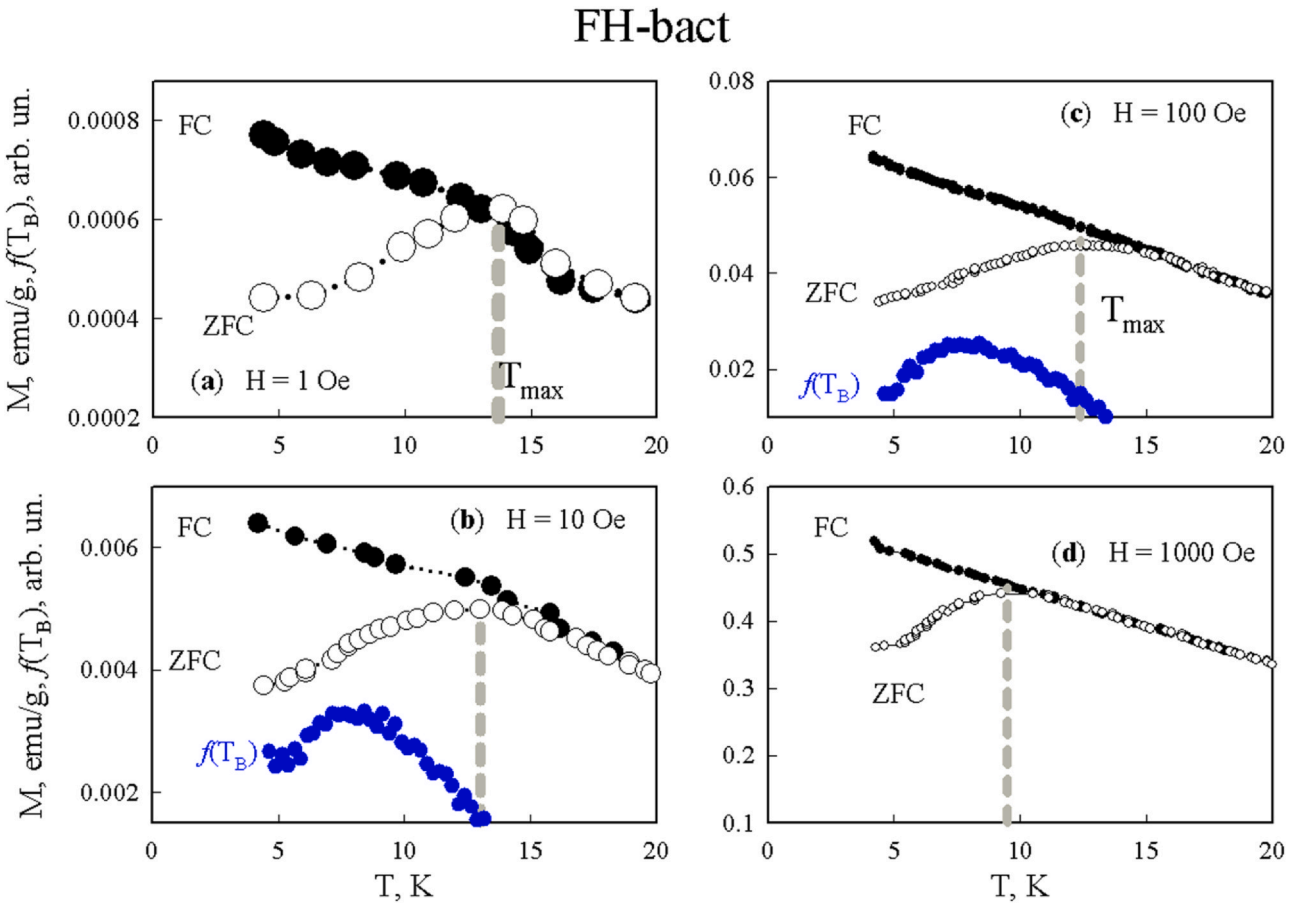

Fig. 5. FC and ZFC M(T) dependences for sample FH-bact in different fields H. Vertical dashed lines correspond to temperatures T_{max} in the $M(T)_{ZFC}$ dependences. (b, c) Dependences $f(T_B) \sim d(M(T)_{ZFC} - M(T)_{FC}/dT)$ (arbitrary units).

increase in the external field from 1 Oe to 1 kOe, i.e., in contrast to synthetic ferrihydrite, decreases by ~40% from the value at H = 1 Oe.

The other striking difference is observed between the $M(T)_{FC}$ dependences. For sample FH-chem, the $M(T)_{FC}$ dependences obtained in fields of 1, 10, 100, and 1000 Oe have maxima at the same temperatures T_{max} as the $M(T)_{ZFC}$ dependences in Fig. 5; consequently, the $M(T)_{FC}$ dependences in the range of $T < T_{max}$ are nonmonotonic. At the same time, the $M(T)_{FC}$ dependences of sample FH-bact (Fig. 5) monotonically increase with decreasing temperature. Qualitatively, the above-described behavior of the $M(T)_{ZFC}$ and $M(T)_{FC}$ dependences of sample FH-bact is typical of SPM blocking of the systems of noninteracting particles.

The above-mentioned difference between the behaviors of the M(T) dependences of the chemical and biogenic ferrihydrite samples and the great difference between the T_{max} values (44 K for FH-chem and 13.7 K for FH-bact-1) in a weak (1 Oe) field cannot be explained by the small difference between the medium ($< d > \approx 2.7$ and 2.2 nm) or maximum (~3 and 3.3 nm) particle sizes (Fig. 1). Obviously, the behavior observed for sample FH-chem is caused by the presence of magnetic interactions.

3.3. Character of the transition from the blocked to SPM state according to the Mössbauer spectra

Fig. 6 shows Mössbauer spectra of the synthetic ferrihydrite sample in the temperature range of 4–300 K. At room temperature, the spectrum represents a paramagnetic doublet consisting of three components corresponding to the three nonequivalent iron positions found earlier [7,66–69]. This doublet is indicative of the SPM state of the magnetic moments of iron cations. The latter are in the high-spin trivalent state in all the positions. The ratio between the relative areas of these components in the spectrum is approximately 3: 2: 1 and almost does not change over the entire temperature range (see Table 1). A decrease in temperature leads to the appearance of a hyperfine structure of the spectrum. When the magnetic state of nanoparticles is established, the relaxation behavior occurs and the shape of the spectra becomes typical of systems of interacting particles [10,70,71]. The Mössbauer spectra show the complete Zeeman splitting (sextets) only below 40 K. The fully unblocked (SPM) state of particles (doublet) is observed at 90 K and above.

In the temperature range of 40–90 K, the Mössbauer spectra of sample FH-chem exhibit the characteristic non-Lorentzian broadening of the sextet lines. Here, it is useful to compare the data obtained with the spectra for sample FH-bact from [49] (See Fig. S.1). For this sample, which has a similar particle size distribution, the spectra were separated, with good accuracy, into partial components – doublet and sextet – with the relative fractions mutually redistributed from 100% to zero, respectively, with a decrease in temperature from 40 to 4 K [49]. The mentioned temperature evolution of the Mössbauer spectra is typical for separated particles, as shown in numerous papers [10,25,42,71]. Furthermore, such a case allows the estimation of the particle size distribution, as it was carried out for a biogenic sample [49]. At the same time, isolated particles in this sample provide a huge surface contribution that does not permit the distinction of nonequivalent iron states, unlike FH-chem.

We note that polysaccharide-coated particles in FH-bact show a narrower blocking process of magnetic moments, that occurs in the range of 10–30 K. In contrast, the sample FH-chem in the temperature range of 40–90 K (Fig. 6) demonstrates a relaxation component and nonuniform broadening of the sextet lines. The relaxation

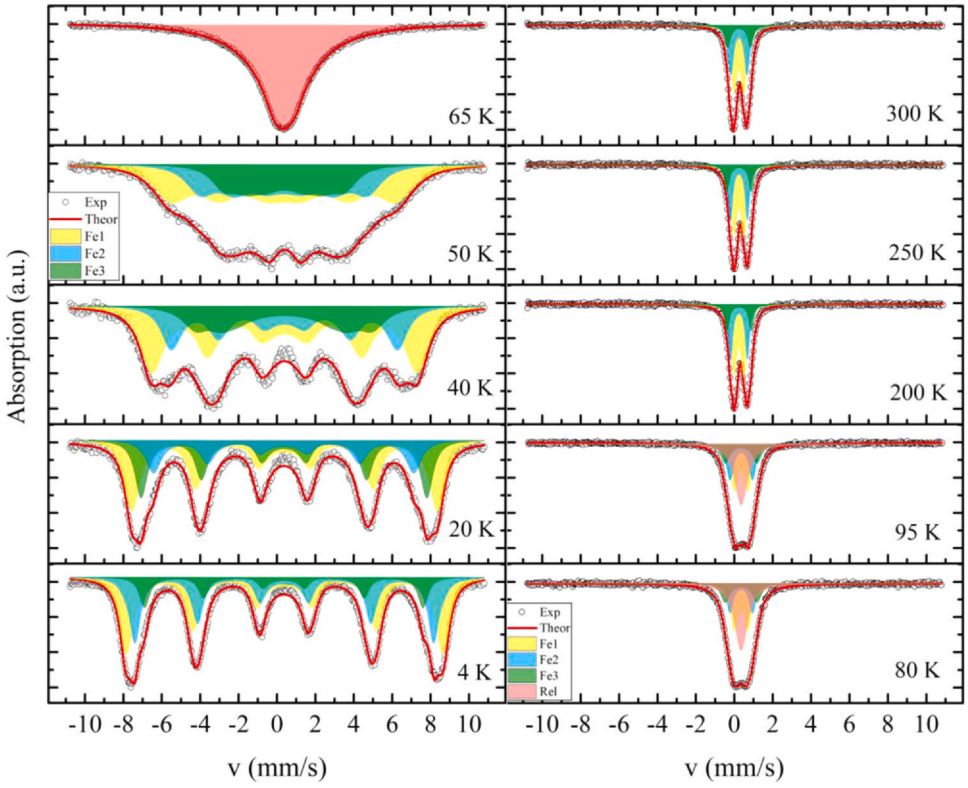

Fig. 6. Mössbauer spectra of sample FH-chem obtained in the temperature range of 4–300 K. Spectral components are painted by colors according to the legends. The relaxation spectra were processed using the model from [53,54] (solid lines).

Table 1
Mössbauer parameters of chemical ferrihydrite nanoparticles in the temperature range of 4–300 K. Chemical shifts are given relative to α-Fe.

	IS, ± 0.005 mm/s	H_{hf}, ± 3 kOe	QS, ± 0.01 mm/s	W, ± 0.01 mm/s	$\tau \cdot 10^{-8}$, s	A, ± 0.03%
4 K						
1	0.512	512	0	–	4.0	0.47
2	0.498	485	0	–	4.9	0.34
3	0.47	452	0	–	4.8	0.18
20 K						
1	0.507	493	0	–	3.5	0.45
2	0.482	463	0	–	4.3	0.32
3	0.466	423	0	–	3.4	0.24
25 K						
1	0.506	480	0	–	2.9	0.47
2	0.485	445	0	–	3.7	0.31
3	0.479	397	0	–	3.0	0.21
–	–	–	–	–	–	–
40 K						
1	0.506	430	0	–	2.0	0.48
2	0.5	368	0	–	2.2	0.30
3	0.506	255	0	–	1.9	0.23
50 K						
1	0.452	368	0.008	–	1.2	0.46
2	0.462	269	0	–	1.4	0.34
3	0.511	186	0	–	1.8	0.20
65 K						
1	0.482	253	0.067	–	0.19	0.99
250 K						
1	0.388	–	0.47	0.31	–	0.48
2	0.391	–	0.92	0.28	–	0.30
3	0.399	–	1.47	0.29	–	0.20
300 K						
1	0.358	–	0.47	0.37	–	0.45
2	0.361	–	0.82	0.30	–	0.38
3	0.373	–	1.17	0.32	–	0.17

behavior and much higher blocking temperature coincide with the previous Mössbauer observation of the interacting nanoparticles [10,42,71]. Thus, we relate the appearance of a distinct relaxation FH-chem spectra with the interparticle interactions.

4. Discussion

4.1. Estimating characteristic parameters of the magnetic interactions and SPM blocking temperature

We can make the estimation that will disclose the presence of magnetic interactions in magnetic nanoparticle systems. The average uncompensated magnetic moment of particles in the synthetic ferrihydrite sample is ≈ 174 μ_B and the corresponding magnetization M_{FM} is ~ 6 emu/g (Fig. 3b). Taking the physical density to be ≈ 4 g/cm^3, we find 4πM ≈ 300 Gs. This, in fact, is the field induced by each particle on its surface ("magnetic pole") with disregard of the external field (the uncompensated magnetic moment of a particle exists even without applied field). Under the conditions of contacts between neighboring particles, each particle is already in a certain spatially nonuniform field, which is a superposition of the external and induced fields. Certainly, this cannot but affect the behavior of the M(T) dependences, especially if the external field is of the same order of magnitude as the value 4π***M*** (considering already several nearest neighboring particles). The aforesaid qualitatively explains the invariability of temperature T_{max} with an increase in the external field from 1 Oe to 1 kOe for sample FH-chem, which is atypical of the SPM blocking.

The presence of a maximum at the same temperature T_{max} as the $M(T)_{ZFC}$ maximum or the appearance of characteristic bends in the $M(T)_{FC}$ dependences is usually attributed to the effect of the interparticle magnetic interactions [28,72–78]. This behavior is observed in sample FH-chem.

The energy kT_{ip} of magnetic interactions between nanoparticles with magnetic moment μ_P is conventionally estimated using the classical equation of electrostatics [10].

$$T_{ip} \approx N_n \mu_P^2/d_{p\text{-}p}^3 \text{ k} \quad (3)$$

At $\mu_P = <\mu_{un}> = 170\ \mu_B$, $d_{p\text{-}p} = <d>$, and the number $N_n = 6$ of the nearest neighbors, Eq. (3) yields a T_{ip} value of about 7 K. This is multiplied lower than the energy of interparticle interactions in ferrimagnetic nanoparticles with typical parameters of $d_{p\text{-}p} \approx 6$ nm and $\mu_P \sim 10^3\ \mu_B$ (see, for example, [10,74,79]), but significantly exceeds this quantity for ferritin ($T_{ip} \approx 0.3$ K at $d_{p\text{-}p} \approx 8$ nm and $<\mu_{un}> = 200\ \mu_B$). Concerning sample FH-bact, the presence of an organic shell of particles with a thickness of only 1 nm and, correspondingly, an increase in $d_{p\text{-}p}$ to 4 nm, will lead to a decrease in T_{ip}, already down to 1.7 K. Therefore, the interparticle magnetic interactions in synthetic ferrihydrite can significantly affect the behavior of its magnetic properties.

Let us turn to the processes of SPM blocking/unblocking of the magnetic moments of particles for different experimental techniques. These processes are described in the Néel–Brown consideration and the SPM blocking temperature is determined as.

$$T_B = K_{eff}V/\ln(\tau_m/\tau_0)\ \text{k} \cdot \quad (4)$$

Here, K_{eff} is the effective magnetic anisotropy constant, which includes the bulk magnetic anisotropy, shape anisotropy and surface effects; V is the particle volume; τ_m is the characteristic measuring time, which depends on the experimental technique used; and τ_0 is the characteristic relaxation time (in the unblocked state, τ_0 can lie within 10^{-9}–10^{-13} s) [10]. Eq. (4) is applicable to the systems of noninteracting particles. In such systems, the particle blocking processes are only determined by the magnetic anisotropy and particle size and, in fact, the magnetic moment of particles under the FC conditions is frozen along the selected spatial direction (along the easy magnetization axis in a nanocrystal) corresponding to the minimum energy.

In [49], the real particle size distribution for sample FH-bact was compared with the SPM blocking temperatures determined from the Mössbauer spectra and the M(T) dependences. In the first case, relative fractions of the doublet (unblocked state) and sextet (blocked state) at different temperatures (4–40 K) were analyzed, which allowed us to determine the blocking temperature distribution function $f(T_B)_{MS}$. The magnetic properties were analyzed based on the well-known fact about the proportionality of the dependence $d(M(T)_{ZFC}–M(T)_{FC}/dT)$ of the blocking temperature distribution function $f(T_B)_{MAGN}$ [66,68,72,80,81]. Fig. 5b and c show the example of the dependences $f(T_B)_{MAGN} \sim d(M(T)_{ZFC}–M(T)_{FC}/dT)$. The agreement between the $f(T_B)_{MS}$ and $f(T_B)_{MAGN}$ functions and the $f(d)$ distribution (Fig. 1) in the framework of Eq. (4) was obtained taking into account that the effective magnetic anisotropy depends on the particle size as.

$$K_{eff} = K_1 + 6\,K_S/d \cdot \quad (5)$$

Here, $K_1 = K_V(1 + K_C/K_V)^2/4$ accounts for both, the bulk (K_V) and shape anisotropy (K_C) of the material [84], and K_S is the surface magnetic anisotropy. K_1 and K_S for the biogenic sample were obtained from experimental data in [49]. The following values are $K_1 = 1.2{\cdot}10^5$ erg/cm^3 and $K_S = 0.1$ erg/cm^2. Shape anisotropy of the particles quite is possible and may give a huge contribution into the K_{eff} value. However, rod-type particles are not observed in our micrographs. Nevertheless, the quasi-spherical shape of particles is not excluded, but according to the term KC/KV in expression for K1, the effect of shape is not dominating.

A similar analysis for sample FH-chem is complicated due to the following points. First, according to the $M(T)_{FC}$ and $M(T)_{ZFC}$ data, the dependences $d(M(T)_{ZFC} - M(T)_{FC}/dT)$ are complex nonmonotonic functions (Fig. 4b, c) and, second, the relaxation behavior of the MS spectra (Fig. 6) is observed, and this is due to the interparticle magnetic interactions.

Moreover, if we attempt to estimate the τ_0 parameter in the Néel–Brown approximation (Eq. (4)), using the obtained parameters of the "blocking temperature" ($T_B = T_{max} \approx 44$ (the magnetic measurements, Fig. 4) and $T_B \approx 90$ K (according to the MS data)), which correspond to the largest particles, then we obtain a nonphysical short particle relaxation time of $\tau_0 \approx 4{\cdot}10^{-18}$ s. This is indicative of the presence of the interparticle magnetic interactions in sample FH-chem [84]. Hence, a more complicated model should be used to consider interparticle interactions. Eq. (4) may be modified accounting the well-known Vogel–Fulcher law on the relaxation time (Eq. 6), which considers the interaction energy on the relaxation time [84].

$$(T_B - T_0) = K_{eff}V/\ln(\tau_m/\tau_0)\ \text{k} \cdot \quad (6)$$

Here, the parameter T_0 determines the degree of interparticle interactions, which are fairly strong at T_0 comparable with T_B [72,75–79,36]. Our estimation of the relaxation time using Eq. (6) gives the reasonable value of $\tau_0 = 4{\cdot}10^{-11}$ s that corresponds to $T_0 = 35$ K.

4.2. Manifestation of collective effects in the temperature evolution of the Mössbauer spectra

A manifestation of the interparticle magnetic interactions can be the fundamentally different character of the magnetic moments blocking of particles with decreasing temperature [82,83,72–79]. Here, instead of SPM blocking, it would be reasonable to speak about freezing of the magnetic moments of particles and the magnetic moment of a particle may tend to occupy a position that does not

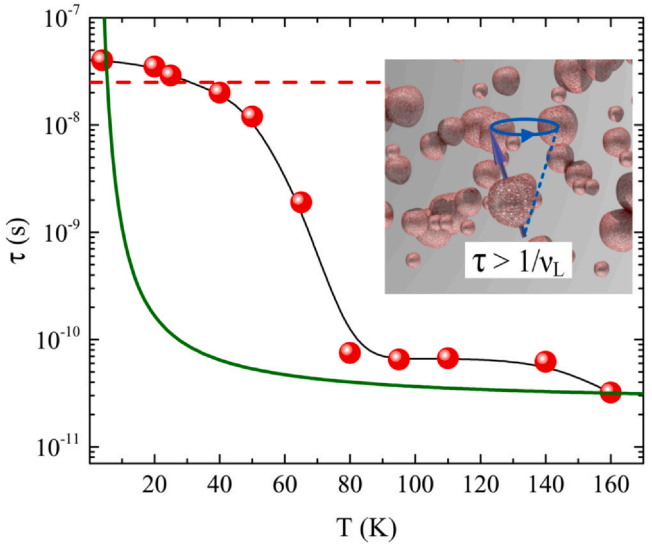

Fig. 7. Temperature dependence of the relaxation time τ of the particle magnetic moments for sample FH-chem. The dotted line shows the characteristic Mössbauer spectroscopy measurement time $1/\nu_L \approx 2.5 \cdot 10^{8-}$ s. Black solid line is drawn by eye. The bold green line represents the result of the theoretical calculation in the Néel–Brown approximation.

necessarily correspond to the minimum magnetic anisotropy. For such a state of the system, the term spin-glass-like is also more appropriate; but, here, the glass state of the magnetic moments of particles is meant [72–79].

In view of the aforesaid, the Mössbauer spectra in Fig. 6 were processed using the model from [53,54], which allows us to extract the particle relaxation time τ at a fixed temperature. The fitting results are shown by solid lines in Fig. 6. Fig. 7 shows the temperature dependence of the particle relaxation time (the average value was taken). Note the growth of the τ_0 value by more than two orders of magnitude in the temperature range of 80–40 K, in which the Mössbauer spectrum is already represented by a single broad line. The dashed horizontal line in Fig. 7 shows the characteristic measuring time $\tau_m = \tau_{MS} \approx 2.5 \cdot 10^{8-}$ s. In the range of 30–40 K, the average particle relaxation time is similar to the value ν_L of the Larmor precession of the iron nucleus. Note that, for the data in the temperature range of 4–20 K, the model from [53,54] only allows us to conclude that $\tau > 1/\nu_L$ and the τ values can be larger. Above 80 K, the model from [53,54] identifies the transition of the sample to the SPM state with the parameters typical of the room-temperature measurements (Table 1).

The main conclusion following from the analysis of the Mössbauer spectra within the model from [53,54] is a significant increase in the particle relaxation time τ with a decrease in temperature in a certain range, which, in comparison with the data on the bacterial ferrihydrite sample [49], indicates the collective processes of freezing of the particle magnetic moments in synthetic ferrihydrite.

Note that a decrease in the particle relaxation time does not drastically affect the estimation of T_0 within the framework of expression (6). If the value $\tau \sim 2 \cdot 10^{-8}$ s (average value for the temperature range 40–50 K) is used in expression (6) instead of τ_0, then for static magnetic measurements ($\tau_m = \tau_{MAGN} = 10^2$ s) the T_B value will be 44 K (coincide with $T_{max} \approx 44$ K, Fig. 3a–d) at $T_0 \approx 22$ K.

5. Conclusions

The main result of this study can be considered the distinguished effect of the interparticle magnetic interactions on the nature of the transition to the unblocked (superparamagnetic) state of the magnetic moments of synthetic ferrihydrite nanoparticles. This result was obtained using the comparative analysis of the magnetic properties (the temperature dependence of the magnetization) and Mössbauer spectra for two samples with the similar particle size distributions: synthetic and biogenic ferrihydrite. In biogenic ferrihydrite, the polysaccharide shell on the particle surface screens the interparticle magnetic interactions. For this sample, the behavior of the M(T) dependences at different thermomagnetic prehistories is typical of systems of noninteracting magnetic particles. The analysis of the M(T) dependences and Mössbauer spectra makes it possible to compare the SPM blocking temperature distribution functions with the particle size distribution and determine the parameters characterizing ferrihydrite (bulk and surface magnetic antitropy constants K_V and K_S). The M(T) dependences for the synthetic ferrihydrite sample have the features attributed to the interparticle magnetic interactions. These are (i) the independence of temperature T_{max} (the $M(T)_{ZFC}$ maximum) of the external field in fields from 1 to ~10^3 Oe, (ii) the nonmonotonic behavior of the $M(T)_{FC}$ dependences, and (iii) somewhat overestimated SPM blocking temperature, under the assumption $T_{max} = T_B$. The latter is confirmed by the analysis of the temperatures of the transition to the unblocked state based on the magnetic and Mössbauer spectroscopy data using the Néel–Brown relation, which yields a nonphysically short particle relaxation time τ_0, which indirectly indicates the contribution of the interparticle interactions. In the Mössbauer spectra in the region of the transition from the SPM (doublet) to the blocked (sextet) state, the interparticle interactions are reflected in the large contribution of the relaxation component and nonuniform broadening of the sextet lines. This complicates the description of the spectra in a standard way, in which the partial components of the spectra (doublet and sextet) correspond to the relative number of unblocked and blocked particles. The processing of the Mössbauer spectra using the model from [53,54] allowed us to extract the particle relaxation time τ. The obtained temperature dependence of the relaxation time reveals freezing of the magnetic moments of particles with decreasing temperature (Fig. 7). These results are indicative of the predominantly collective processes of freezing of the magnetic moments of particles, which is caused by the interparticle magnetic interactions in synthetic ferrihydrite.

Funding

This study was supported by the Russian Foundation for Basic Research, the Government of the Krasnoyarsk Territory, and the Krasnoyarsk Territorial Foundation for Support of Scientific and R&D Activities, project no. 19–42–240012 R-A "Magnetic Resonance in Ferrihydrite Nanoparticles: Effects Related to the Core-Shell Structure".

CRediT authorship contribution statement

Yu. V. Knyazev: Writing – original draft, Data curation, Formal analysis, Investigation, Visualization, Writing – review & editing. **D. A. Balaev:** Conceptualization, Investigation, Data curation, Funding acquisition, Visualization, Writing – original draft, Methodology, Software, Writing – review & editing. **S. V. Stolyar:** Investigation, Funding acquisition. **A. A. Krasikov:** Investigation, Data curation. **O. A. Bayukov:** Validation, Software, Formal analysis, Investigation, Software. **M. N. Volochaev:** Investigation, Visualization. **R. N. Yaroslavtsev:** Investigation, Visualization. **V. P. Ladygina:** Investigation, Software. **D. A. Velikanov:** Investigation, Software. **R. S. Iskhakov:** Supervision.

Declaration of Competing Interest

The authors declare that they have no known competing financial interests or personal relationships that could have appeared to influence the work reported in this paper.

Acknowledgments

The electron microscopy study was carried out on the equipment of the Krasnoyarsk Territorial Center for Collective Use, Krasnoyarsk Scientific Center, Siberian Branch of the Russian Academy of Sciences.

Appendix A. Supporting information

Supplementary data associated with this article can be found in the online version at doi:10.1016/j.jallcom.2021.161623.

References

[1] P.F. Lindley, Iron in biology: a structural viewpoint, Rep. Prog. Phys. 59 (1996) 867–933, https://doi.org/10.1088/0034-4885/59/7/002
[2] J.L. Jambor, J.E. Dutrizac, Occurrence and constitution of natural and synthetic ferrihydrite, a widespread iron oxyhydroxide, Chem. Rev. 98 (7) (1998) 2549–2585, https://doi.org/10.1021/cr970105t
[3] S.V. Stolyar, D.A. Balaev, V.P. Ladygina, A.A. Dubrovskiy, A.A. Krasikov, S.I. Popkov, O.A. Bayukov, Yu.V. Knyazev, R.N. Yaroslavtsev, M.N. Volochaev, R.S. Iskhakov, K.G. Dobretsov, E.V. Morozov, O.V. Falaleev, E.V. Inzhevatkin, O.A. Kolenchukova, I.A. Chizhova, Bacterial ferrihydrite nanoparticles: preparation, magnetic properties, and application in medicine, J. Supercond. Nov. Magn. 31 (2018) 2297–2304, https://doi.org/10.1007/s10948-018-4700-1
[4] S.V. Stolyar, V.P. Ladygina, A.V. Boldyreva, O.A. Kolenchukova, A.M. Vorotynov, M.S. Bairmani, R.N. Yaroslavtsev, R.S. Iskhakov, Synthesis, properties, and in vivo testing of biogenic ferrihydrite nanoparticles, Bull. Russ. Acad. Sci.: Phys. 84 (11) (2020) 1366–1369, https://doi.org/10.3103/S106287382011026X
[5] M. Mohapatra, D. Hariprasad, L. Mohapatra, S. Anand, B. Mishra, Mg-doped nano ferrihydrite––a new adsorbent for fluoride removal from aqueous solutions, Appl. Surf. Sci. 258 (10) (2012) 4228–4236, https://doi.org/10.1016/j.apsusc.2011.12.047
[6] F.M. Michel, L. Ehm, S.M. Antao, P.L. Lee, P.J. Chupas, G. Liu, D.R. Strongin, M.A.A. Schoonen, B.L. Phillips, J.B. Parise, The structure of ferrihydrite, a nanocrystalline material, Science 316 (2007) 1726–1729, https://doi.org/10.1126/science.1142525
[7] S. Stolyar, O. Bayukov, D. Balaev, R. Iskhakov, L. Ishchenko, V. Ladygina, R. Yaroslavtsev, et al., Production and magnetic properties of biogenic ferrihydrite nanoparticles, J. Optoelectron. Adv. Mater. 17 (2015) 968–972.
[8] V. Ladygina, K. Purtov, S. Stoljar, R. Iskhakov, O. Bajukov, G. Gurevich, K. Dobretsov, I. La, Method of Producing Stable Aqueous Sol Based on Ferrihydrite Nanoparticles, 2013 Russian EA018956.
[9] M. Seehra, V.S. Babu, A. Manivannan, J. Lynn, Neutron scattering and magnetic studies of ferrihydrite nanoparticles, Phys. Rev. B B 61 (5) (2000) 3513–3518, https://doi.org/10.1103/PhysRevB.61.3513
[10] S. Mørup, D.E. Madsen, C. Fradsen, C.R.H. Bahl, M.F. Hansen, Experimental and theoretical studies of nanoparticles of antiferromagnetic materials, J. Phys.: Condens. Matter 19 (2007) 213202, https://doi.org/10.1088/0953-8984/19/21/213202
[11] Y.L. Raikher, V. Stepanov, Magneto-orientational behavior of a suspension of antiferromagnetic particles, J. Phys. Condens. Matter 20 (20) (2008) 204120, https://doi.org/10.1088/0953-8984/20/20/204120
[12] L. Néel, Superparamagnétisme des grains très fins antiferromagnétiques, C. R. Acad. Sci. Paris 252 (1961) 4075.
[13] S.A. Makhlouf, F.T. Parker, A.E. Berkowitz, Magnetic hysteresis anomalies in ferritin, Phys. Rev. B 55 (1997) R14717–R14720.
[14] C. Gilles, P. Bonville, K.K.W. Wong, S. Mann, Non-Langevin behaviour of the uncompensated magnetization in nanoparticles of artificial ferritin, Eur. Phys. J. B 17 (2000) 417–427.
[15] C. Gilles, P. Bonville, H. Rakoto, J.M. Broto, K.K.W. Wong, S. Mann, Magnetic hysteresis and superantiferromagnetism in ferritin nanoparticles, J. Magn. Magn. Mater. 241 (2002) 430–440, https://doi.org/10.1016/S0304-8853(01)00461-9
[16] A. Punnoose, T. Phanthavady, M. Seehra, N. Shah, G. Huffman, Magnetic properties of ferrihydrite nanoparticles doped with Ni, Mo, and Ir, Phys. Rev. B 69 (5) (2004) 054425, https://doi.org/10.1103/PhysRevB.69.054425
[17] N.J.O. Silva, V.S. Amaral, L.D. Carlos, Relevance of magnetic moment distribution and scaling law methods to study the magnetic behavior of antiferromagnetic nanoparticles: application to ferritin, Phys. Rev. B 71 (2005) 1844080.1103/PhysRevB.71.184408.
[18] D.A. Balaev, A. Dubrovskii, A. Krasikov, S.V. Stolyar, R.S. Iskhakov, V.P. Ladygina, E. Khilazheva, Mechanism of the formation of an uncompensated magnetic moment in bacterial ferrihydrite nanoparticles, JETP Lett. 98 (3) (2013) 139–142, https://doi.org/10.1134/S0021364013160029
[19] D.A. Balaev, A.A. Krasikov, A.A. Dubrovskii, S.V. Semenov, O.A. Bayukov, S.V. Stolyar, R.S. Iskhakov, V.P. Ladygina, L.A. Ishchenko, Magnetic properties and the mechanism of formation of the uncompensated magnetic moment of antiferromagnetic ferrihydrite nanoparticles of a bacterial origin, J. Exp. Theor. Phys. 119 (3) (2014) 479–487, https://doi.org/10.1134/S1063776114080044
[20] C. Rani, S. Tiwari, Superparamagnetic behavior of antiferromagnetic six lines ferrihydrite nanoparticles, Phys. B Condens. Matter 513 (2017) 58–61, https://doi.org/10.1016/j.physb.2017.02.036
[21] C. Rani, S. Tiwari, Estimation of particle magnetic moment distribution for antiferromagnetic ferrihydrite nanoparticles, J. Magn. Magn. Mater. 385 (2015) 272–276, https://doi.org/10.1016/j.jmmm.2015.02.048
[22] K. Dobretsov, S. Stolyar, A. Lopatin, Magnetic nanoparticles: a new tool for antibiotic delivery to sinonasal tissues. Results of preliminary studies, Acta Otorhinolaryngol. Ital. 35 (2) (2015) 97–102.
[23] E.V. Inzhevatkin, O.A. Kolenchukova, K.G. Dobretsov, V.P. Ladygina, A.V. Boldyreva, S.V. Stolyar, Efficiency of ampicillin-associated biogenic ferrihydrite nanoparticles in combination with a magnetic field for local treatment of burns, Bull. Exp. Biol. Med. 169 (2020) 683–686, https://doi.org/10.1007/s10517-020-04954-y
[24] Y.A. Urian, J.J. Atoche-Medrano, Luis T. Quispe, L. León Félix, J.A.H. Coaquira, Study of the surface properties and particle-particle interactions in oleic acid-coated Fe3O4 nanoparticles, J. Magn. Magn. Mater. 525 (2021) 167686, https://doi.org/10.1016/j.jmmm.2020.167686
[25] S. Mørup, M.F. Hansen, C. Frandsen, Magnetic interactions between nanoparticles, Beilstein J. Nanotechnol. 1 (2010) 182–190, https://doi.org/10.3762/bjnano.1.22
[26] O. Petracic, Superparamagnetic nanoparticle ensembles, Superlattices Microstruct. 47 (2010) 569–578, https://doi.org/10.1016/j.spmi.2010.01.009
[27] J.C. Denardin, A.L. Brandl, M. Knobel, P. Panissod, A.B. Pakhomov, H. Liu, X.X. Zhang, Thermoremanence and zero-field-cooled/field-cooled magnetization study ofCox(SiO2)1−xgranular films, Phys. Rev. B. 65 (2002) 064422, https://doi.org/10.1103/PhysRevB.65.064422
[28] K. Nadeem, H. Krenn, T. Traussnig, R. Würschum, D.V. Szabó, I. Letofsky-Papst, Effect of dipolar and exchange interactions on magnetic blocking of maghemite nanoparticles, J. Magn. Magn. Mater. 323 (2011) 1998–2004, https://doi.org/10.1016/j.jmmm.2011.02.041
[29] V. Russier, Blocking temperature of interacting magnetic nanoparticles with uniaxial and cubic anisotropies from Monte Carlo simulations, J. Magn. Magn. Mater. 409 (2016) 50–55, https://doi.org/10.1016/j.jmmm.2016.02.070
[30] M. Knobel, W.C. Nunes, H. Winnischofer, T.C.R. Rocha, L.M. Socolovsky, C.L. Mayorga, D. Zanchet, Effects of magnetic interparticle coupling on the blocking temperature of ferromagnetic nanoparticle arrays, J. Non Cryst. Solids 353 (2007) 743–747, https://doi.org/10.1016/j.jnoncrysol.2006.12.037
[31] P. Allia, G. Barrera, P. Tiberto, T. Nardi, Y. Leterrier, M. Sangermano, Fe3O4 nanoparticles and nanocomposites with potential application in biomedicine and in communication technologies: nanoparticle aggregation, interaction, and effective magnetic anisotropy, J. Appl. Phys. 116 (2014) 113903, https://doi.org/10.1063/1.4895837
[32] G.F. Goya, T.S. Berquó, F.C. Fonseca, M.P. Morales, Static and dynamic magnetic properties of spherical magnetite nanoparticles, J. Appl. Phys. 94 (2003) 3520–3528, https://doi.org/10.1063/1.1599959
[33] S.B. Trisnanto, Y. Takemura, Dipolar field-induced asymmetric magnetization hysteresis of immobile superparamagnetic nanoclusters, J. Magn. Magn. Mater. 480 (2019) 132–137, https://doi.org/10.1016/j.jmmm.2019.02.077
[34] J.J.A. Medrano, F.F.H. Aragón, L. Leon-Felix, J.A.H. Coaquira, A.F.R. Rodríguez, F.S.E.D.V. Faria, M.H. Sousa, J.C. Mantilla Ochoa, P.C. Morais, Evidence of particle-particle interaction quenching in nanocomposite based on oleic acid-coated Fe3O4 nanoparticles after over-coating with essential oil extracted from Croton cajucara Benth, J. Magn. Magn. Mater. 466 (2018) 359–367, https://doi.org/10.1016/j.jmmm.2018.07.036
[35] M. Vasilakaki, F. Gemenetzi, E. Devlin, D.K. Yi, S.N. Riduan, S.S. Lee, J.Y. Ying, G.C. Papaefthymiou, K.N. Trohidou, Size effects on the magnetic behavior of γ-Fe2O3 core/SiO2 shell nanoparticle assemblies, J. Magn. Magn. Mater. 522 (2021) 167570, https://doi.org/10.1016/j.jmmm.2020.167570
[36] D.A. Balaev, S.V. Semenov, A.A. Dubrovskiy, S.S. Yakushkin, V.L. Kirillov, O.N. Martyanov, Superparamagnetic blocking of an ensemble of magnetite nanoparticles upon interparticleinteractions, J. Magn. Magn. Mater. 440 (2017) 199–202, https://doi.org/10.1016/j.jmmm.2016.12.046
[37] J. Mohapatra, M. Xing, J.P. Liu, Inductive thermal effect of ferrite magnetic nanoparticles, Materials 12 (2019) 3208, https://doi.org/10.3390/ma12193208
[38] S.V. Komogortsev, R.S. Iskhakov, V.A. Fel'k, Fractal dimension effect on the magnetization curves of exchange-coupled clusters of magnetic nanoparticles, J. Exp. Theor. Phys. 128 (2019) 754–760, https://doi.org/10.1134/S1063776119040095
[39] S.V. Komogortsev, V.A. Fel'k, O.A. Li, The magnetic dipole-dipole interaction effect on the magnetic hysteresis at zero temperature in nanoparticles randomly dispersed within a plane, J. Magn. Magn. Mater. 473 (2019) 410–415, https://doi.org/10.1016/j.jmmm.2018.10.091
[40] J. Fock, M.F. Hansen, C. Frandsen, S. Mørup, On the interpretation of Mössbauer spectra of magnetic nanoparticles, J. Magn. Magn. Mater. 445 (2018) 11–21, https://doi.org/10.1016/j.jmmm.2017.08.070
[41] N. Rinaldi-Montes, P. Gorria, D. Martínez-Blanco, A.B. Fuertes, L. Fernández Barquín, I. Puente-Orench, J.A. Blanco, Scrutinizing the role of size reduction on the exchange bias and dynamic magnetic behavior in NiO nanoparticles, Nanotechnology 26 (2015) 305705, https://doi.org/10.1088/0957-4484/26/30/305705

[42] F. Bødker, M.F. Hansen, C. Bender Koch, S. Mørup, Particle interaction effects in antiferromagnetic NiO nanoparticles, J. Magn. Magn. Mater. 221 (2000) 32–36, https://doi.org/10.1016/S0304-8853(00)00392-9

[43] E. Winkler, R.D. Zysler, M. Vasquez Mansilla, D. Fiorani, Surface anisotropy effects in NiO nanoparticles, Phys. Rev. B B 72 (2005) 132409, https://doi.org/10.1103/PhysRevB.72.132409

[44] E. Winkler, R.D. Zysler, M. Vasquez Mansilla, D. Fiorani, D. Rinaldi, M. Vasilakaki, K.N. Trohidou, Surface spin-glass freezing in interacting core–shell NiO nanoparticles, Nanotechnology 19 (2008) 185702, https://doi.org/10.1088/0957-4484/19/18/185702

[45] H. Shim, P. Dutta, M.S. Seehra, J. Bonevich, Size dependence of the blocking temperatures and electron magnetic resonance spectra in NiO nanoparticles, Solid State Commun. 145 (2008) 192–196, https://doi.org/10.1016/j.ssc.2007.10.026

[46] M. Tadic, D. Nikolic, M. Panjan, G.R. Blake, Magnetic properties of NiO (nickel oxide) nanoparticles: blocking temperature and Neel temperature (dx.doi.org/), J. Alloy. Compd. 647 (2015) 1061–1068, https://doi.org/10.1016/j.jallcom.2015.06.027

[47] E.L. Duarte, R. Itri, E. Lima Jr., M.S. Baptista, T.S. Berquó, G.F. Goya, Large magnetic anisotropy in ferrihydrite nanoparticles synthesized from reverse micelles, Nanotechnology 17 (2006) 5549–5555, https://doi.org/10.1088/0957-4484/17/22/004

[48] T.S. Berquó, J.J. Erbs, A. Lindquist, R.L. Penn, S.K. Banerjee, Effects of magnetic interactions in antiferromagnetic ferrihydrite particles, J. Phys. Condens Matter 21 (2009) 176005, https://doi.org/10.1088/0953-8984/21/17/176005

[49] Yu.V. Knyazev, D.A. Balaev, S.V. Stolyar, O.A. Bayukov, R.N. Yaroslavtsev, V.P. Ladygina, D.A. Velikanov, R.S. Iskhakov, Magnetic anisotropy and core-shell structure origin of the biogenic ferrihydrite nanoparticles, J. Alloy. Compd. 851 (2021) 156753, https://doi.org/10.1016/j.jallcom.2020.156753

[50] L. Anghel, M. Balasoiu, L.A. Ishchenko, S.V. Stolyar, T.S. Kurkin, A.V. Rogachev, A.I. Kuklin, Y.S. Kovalev, Y.L. Raikher, R.S. Iskhakov, G. Duca, Characterization of bio-synthesized nanoparticles produced by Klebsiella oxytoca, J. Phys.: Conf. Ser. 351 (2012) 012005, https://doi.org/10.1088/1742-6596/351/1/012005

[51] D.A. Velikanov, Squid magnetometer for investigations of the magnetic properties of materials in the temperature range 4.2–370 K, Sib, J. Sci. Technol. 2 (48) (2013) 176.

[52] A.D. Balaev, Yu.V. Boyarshinov, M.M. Karpenko, B.P. Khrustalev, Automated magnetometer with superconducting solenoid, Prib. Tekh. Eksp. 3 (1985) 167.

[53] F. Van der Woude, A.J. Dekker, The relation between magnetic properties and the shape of Mössbauer spectra, Phys. Status Solidi (b) 9 (3) (1965) 775–786, https://doi.org/10.1002/pssb.19650090314

[54] H.H. Wickman, M.P. Klein, D.A. Shirley, Paramagnetic hyperfine structure and relaxation effects in Mössbauer spectra: Fe^{57} in ferrichrome A, Phys. Rev. 152 (1) (1966) 345–357, https://doi.org/10.1103/PhysRev.152.345

[55] R.P. Guertin, N. Harrison, Z.X. Zhou, S. McCall, F. Drymiotis, Very high field magnetization and AC susceptibility of native horse spleen ferritin, J. Magn. Magn. Mater. 308 (2007) 97–100, https://doi.org/10.1016/j.jmmm.2006.05.010

[56] N.J.O. Silva, A. Millan, F. Palacio, E. Kampert, U. Zeitler, V.S. Amaral, Temperature dependence of antiferromagnetic susceptibility in ferritin, Phys. Rev. B 79 (2009) 104405, https://doi.org/10.1103/PhysRevB.79.104405

[57] D.A. Balaev, A.A. Dubrovskiy, A.A. Krasikov, S.I. Popkov, A.D. Balaev, K.A. Shaikhutdinov, V.L. Kirillov, O.N. Martyanov, Magnetic properties of NiO nano particles: Contributions of the antiferromagnetic and ferromagnetic subsystems in different magnetic field ranges up to 250 kOe, Phys. Solid State 59 (2017) 1547–1552.

[58] S.I. Popkov, A.A. Krasikov, S.V. Semenov, A.A. Dubrovskii, S.S. Yakushkin, V.L. Kirillov, O.N. Mart'yanov, D.A. Balaev, General regularities and differences in the behavior of the dynamic magnetization switching of ferrimagnetic ($CoFe_2O_4$) and antiferromagnetic (NiO) nanoparticles, Phys. Solid State 62 (9) (2020) 1518–1524, https://doi.org/10.1134/S1063783420090255

[59] D.A. Balaev, A.A. Krasikov, S.I. Popkov, A.A. Dubrovskiy, S.V. Semenov, D.A. Velikanov, V.L. Kirillov, O.N. Martyanov, Features of the quasi-static and dynamic magnetization switching in NiO nanoparticles: manifestation of the interaction between magnetic subsystems in antiferromagnetic nanoparticles, J. Magn. Magn. Mater. 515 (2020) 167307, https://doi.org/10.1016/j.jmmm.2020.167307

[60] D.A. Balaev, S.I. Popkov, A.A. Krasikov, A.D. Balaev, A.A. Dubrovskiy, S.V. Stolyar, R.N. Yaroslavtsev, V.P. Ladygina, R.S. Iskhakov, Temperature behavior of the antiferromagnetic susceptibility of nanoferrihydrite from the measurements of the magnetization curves in fields of up to 250 kOe, Phys. Solid State 59 (2017) 1940–1946, https://doi.org/10.1134/S1063783417100031

[61] S.I. Popkov, A.A. Krasikov, D.A. Velikanov, V.L. Kirillov, O.N. Martyanov, D.A. Balaev, Formation of the magnetic subsystems in antiferromagnetic NiO nanoparticles using the data of magnetic measurements in fields up to 250 kOe, J. Magn. Magn. Mater. 483 (2019) 21–26, https://doi.org/10.1016/j.jmmm.2019.03.004

[62] S.I. Popkov, A.A. Krasikov, A.A. Dubrovskiy, M.N. Volochaev, V.L. Kirillov, O.N. Martyanov, D.A. Balaev, Size effects in the formation of an uncompensated ferromagnetic moment in NiO nanoparticles, J. Appl. Phys. 126 (2019) 103904, https://doi.org/10.1063/1.5109054

[63] S.D. Tiwari, K.P. Rajeev, Effect of distributed particle magnetic moments on the magnetization of NiO nanoparticles, Solid State Commun. 152 (2012) 1080–1083, https://doi.org/10.1016/j.ssc.2012.03.003

[64] C. Parmar, G.S. Parmar, Structural and magnetic properties of six-line ferrihydrite nanoparticles, J. Supercond. Nov. Magn. 33 (2020) 441–444, https://doi.org/10.1007/s10948-019-05200-x

[65] T. Iimor, Y. Imamoto, N. Uchida, Y. Kikuchi, K. Honda, T. Iwahashi, Y. Ouch, Magnetic moment distribution in nanosized antiferromagnetic NiO, J. Appl. Phys. 127 (2020) 023902, https://doi.org/10.1063/1.5135335

[66] D.A. Balaev, A.A. Krasikov, A.A. Dubrovskiy, S.I. Popkov, S.V. Stolyar, O.A. Bayukov, R.S. Iskhakov, V.P. Ladygina, R.N. Yaroslavtsev, Magnetic properties of heat treated bacterial ferrihydrite nanoparticles, J. Magn. Magn. Mater. 410 (2016) 171–180, https://doi.org/10.1016/j.jmmm.2016.02.059

[67] D.A. Balaev, A.A. Krasikov, A.D. Balaev, S.V. Stolyar, V.P. Ladygina, R.S. Iskhakov, Features of relaxation of the remanent magnetization of antiferromagnetic nanoparticles by the example of ferrihydrite, Phys. Solid State 62 (7) (2020) 1172–1178, https://doi.org/10.1134/S1063783420070033

[68] D.A. Balaev, A.A. Krasikov, S.V. Stolyar, R.S. Iskhakov, V.P. Ladygina, R.N. Yaroslavtsev, O.A. Bayukov, A.M. Vorotynov, M.N. Volochaev, A.A. Dubrovskiy, Change in the magnetic properties of nanoferrihydrite with an increase in the volume of nanoparticles during low-temperature annealing, Phys. Solid State 58 (9) (2016) 1782–1791, https://doi.org/10.1134/S1063783416090092

[69] S.V. Stolyar, R.N. Yaroslavtsev, R.S. Iskhakov, O.A. Bayukov, D.A. Balaev, A.A. Dubrovskii, A.A. Krasikov, V.P. Ladygina, A.M. Vorotynov, M.N. Volochaev, Magnetic and resonance properties of ferrihydrite nanoparticles doped with cobalt, Phys. Solid State 59 (3) (2017) 555–563, https://doi.org/10.1134/S1063783417030301

[70] Y. Guyodo, S.K. Banerjee, R. Lee Penn, D. Burleson, T.S. Berquo, T. Seda, P. Solheid, Magnetic properties of synthetic six-line ferrihydrite nanoparticles, Phys. Earth Planet. Inter. 154 (2006) 222–233, https://doi.org/10.1016/j.pepi.2005.05.009

[71] L. Theil Kuhn, K. Lefmann, C.R.H. Bahl, S. Nyborg Ancona, P.-A. Lindgård, C. Frandsen, D.E. Madsen, S. Mørup, Neutron study of magnetic excitations in8−nmα−Fe2O3nanoparticles, Phys. Rev. B 74 (18) (2006) 184406, https://doi.org/10.1103/PhysRevB.74.184406

[72] C.A.M. Vieira, R. Cabreira Gomes, F.G. Silva, A.L. Dias, R. Aquino, A.F.C. Campos, J. Depeyrot, Blocking and remanence properties of weakly and highly interactive cobalt ferrite based nanoparticles, J. Phys. Condens Matter 31 (2019) 175801, https://doi.org/10.1088/1361-648X/ab0353

[73] M. Suzuki, S.I. Fullem, I.S. Suzuki, L. Wang, C.-J. Zhong, Observation of superspin-glass behavior in Fe3O4 nanoparticles, Phys. Rev. B 79 (2009) 024418, https://doi.org/10.1103/PhysRevB.79.024418

[74] O. Petracic, X. Chen, S. Bedanta, W. Kleeman, S. Sahoo, S. Cardoso, P.P. Freitas, Collective states of interacting ferromagnetic nanoparticles, J. Magn. Magn. Mater. 300 (2006) 192–197, https://doi.org/10.1016/j.jmmm.2005.10.061

[75] J. Mohapatra, A. Mitra, D. Bahadur, M. Aslam, Superspin glass behavior of self-interacting $CoFe_2O_4$ nanoparticles, J. Alloy Comp. 628 (2015) 416–423, https://doi.org/10.1016/j.jallcom.2014.12.197

[76] S.K. Sharma, Ravi Kumar, Shalendra Kumar, M. Knobel, C.T. Meneses, V.V. Siva Kumar, V.R. Reddy, M. Singh, C.G. Lee, Role of interparticle interactions on the magnetic behavior of Mg(0.95)Mn(0.05)Fe(2)O(4) ferrite nanoparticles, J. Phys. Condens Matter 20 (2008) 235214, https://doi.org/10.1088/0953-8984/20/23/235214

[77] Y.A. Urian, J.J. Atoche-Medrano, Luis T. Quispe, L. León Félix, J.A.H. Coaquira, Study of the surface properties and particle-particle interactions in oleic acid-coated Fe3O4 nanoparticles, J. Magn. Magn. Mater. 525 (2021) 167686, https://doi.org/10.1016/j.jmmm.2020.167686

[78] K. Nadeem, M. Kamran, A. Javed, F. Zeb, S.S. Hussain, M. Mumtaz, H. Krenn, D.V. Szaboc, U. Brossmann, Xiaoke Mu, Role of surface spins on magnetization of Cr2O3 coated γ-Fe2O3 nanoparticles, Solid State Sci. 83 (2018) 43–48, https://doi.org/10.1016/j.solidstatesciences.2018.07.006

[79] A.M. Pereira, C. Pereira, A.S. Silva, D.S. Schmool, C. Freire, J.-M. Grenèche, Joao P. Araujo, Unravelling the effect of interparticle interactions and surface spin canting in γ-Fe2O3@SiO2 superparamagnetic nanoparticles, J. Appl. Phys. 109 (2011) 114319, https://doi.org/10.1063/1.3583652

[80] D. Tobia, E. Winkler, R.D. Zysler, M. Granada, H.E. Troiani, D. Fiorani, Exchange bias of Co nanoparticles embedded in Cr2O3 and Al2O3 matrices, J. Appl. Phys. 106 (2009) 103920, https://doi.org/10.1063/1.3259425

[81] J.C. Denardin, A.L. Brandl, M. Knobel, P. Panissod, A.B. Pakhomov, H. Liu, X.X. Zhang, Thermoremanence and zero-field-cooled/field-cooled magnetization study ofCox(SiO2)1−xgranular films, Phys. Rev. B 65 (2002) 064422, https://doi.org/10.1103/PhysRevB.65.064422

[82] J.L. Dormann, D. Fiorani, R. Cherkaoui, E. Tronc, F. Lucari, F. D'Orazio, L. Spinu, M. Noguès, H. Kachkachi, J.P. Jolivet, From pure superparamagnetism to glass collective state in γ-Fe2O3 nanoparticle assemblies, J. Magn. Magn. Mater. 203 (1999) 23–27, https://doi.org/10.1016/S0304-8853(99)00180-8

[83] C. Djurberg, P. Svedlindh, P. Nordblad, M.F. Hansen, F. Bødker, S. Mørup, Dynamics of an interacting particle system: evidence of critical slowing down, Phys. Rev. Lett. 79 (25) (1997) 5154–5157, https://doi.org/10.1103/PhysRevLett.79.5154

[84] J.L. Dormann, L. Bessaist, D. Fiorani, A dynamic study of small interacting particles: superparamagnetic model and spin-glass laws, J. Phys. C: Solid State Phys. 21 (1988) 2015–2034, https://doi.org/10.1088/0022-3719/21/10/019